LA-UR-82-618

Conf-820313--3

Los Alamos National Laboratory is operated by the University of California for the United States Department of Energy under contract W-7405-ENG-36

LA-UR--82-618

DE82 011981

TITLE: THE ACOUSTIC DISTURBANCE AT IONOSPHERIC HEIGHTS CAUSED BY THE MILL RACE EXPLOSION*

AUTHOR(S): [illegible]ght G [illegible] l
David J.

SUBMITTED TO: Defense Nuclear Agency
Mill Race Results Symposium
Adelphi, Maryland
March 16, 17, 18, 1982

*Research performed under the auspices of the United States Department of Energy, International Security Affairs Research and Development Program.

Los Alamos Los Alamos National Laboratory
Los Alamos, New Mexico 87545

CONTENTS

LIST OF ILLUSTRATIONS

LIST OF TABLES

SECTION 1

INTRODUCTION

1-1 GENERAL

The principal objective of the Los Alamos National Laboratory in the MILL RACE experiment was to measure the over-head ionospheric response due to he MILL RACE explosion. Such a measurement enables us to test computer models designed to quantitatively predict ionospheric disturbances caused by known sources. The emphasis of the models has been directed at calculating effects on rf propagation associated with the predicted ionospheric disturbances. Consequently vertical incidence phase sounding measurements of a well-characterized source provide a direct and sensitive test of the computer models and, for this reason, a vertical incidence phase sounder was located 3,300 meters to the west of the MILL RACE ground zero.

Another area of interest is the development of an understanding of the atmospheric response to known sources at distances where the acoustic response no longer dominates. Such an undertaking requires measurements at these remote points. Deployment of a bistatic sounding network enabled us to investigate this area of interest.

1-2 OTHER EXPERIMENTS

Other ionospheric measurements were obtained during the MILL RACE event by NOAA/SEL, UCLA Geophysics Laboratory and SRI. These measurements were vertical incidence phase soundings at remote sites, magnetometer measurements and over-the-horizon radar measurements.

1-3 INQUIRIES

Inquiries are invited and should be directed to either:

D.J. Simons or
D.G. Rickel
Atmospheric Sciences Group, MS 466
Los Alamos National Laboratory
Los Alamos, NM 87545

Telephone: 505-667-1222

SECTION 2

EXPERIMENTAL SPECIFICATIONS

2-1 VERTICAL INCIDENCE PHASE SOUNDER.

The phase sounder was operated at three frequencies in a pulsed mode at an instantaneous power of three kilowatts. A pulse repetition rate of 120 pulses per second was selected which gave a time resolution for ionospheric motions on the order of 10 milliseconds with a range resolution of approximately 15 kilometers. We selected operating frequencies at 5.37, 7.98 and 10.3 Mhz which gave reflection heights of 145, 220 and 260 kilometers respectively. These reflection heights were obtained from electron density profiles deduced from ionograms acquired by the White Sands dynasonde.

On event day the ionospheric conditions were excellent. Very little sporadic E was present and consequently we were able to monitor the selected heights continuously with good signal-to-noise ratio. Data were obtained over continuous 8 hour periods starting at 0800 MDT for September 15,16 and 17, 1981. Analog recordings were made of the receiver signals along with an IRIG time code and a constant frequency reference signal.

2-2 BISTATIC PHASE SOUNDER.

Figure 1 shows the placement of the receiver and the transmitter stations for the bistatic network. A list of the geographic locations of these sites is given in Table 1. It is assumed that most of the rf energy propagated from the transmitters to the receivers would be by a single skip from the ionosphere. This would give us an inspection point of the ionosphere at each of the ionospheric reflection points.

Table 1
Station Locations

Pagosa Springs, CO (receiver)	37° 20′	107° 06′
Monte Vista, CO (transmitter)	37° 34′	106° 09′
Taos, NM (receiver)	36° 22′	105° 30′
Los Alamos, NM (receiver)	35° 52′	106° 22′
Mountainair, NM (receiver)	34° 31′	106° 17′
Stallion Range, NM (transmitter)	33° 50′	106° 40′
MILL RACE Test	33° 37′	106° 28′

Table 2 lists the distances of the reflection points from the MILL RACE ground zero. The placement of the receiver and transmitter stations were not optimal because at the resulting ionospheric reflection points the coupling is weak between the ionospheric electrons and the propagating acoustic disturbance (reference 1). Logistically, however, this was a convenient arrangement.

The Los Alamos transmitters were Collins hf380 transceivers set up in cw mode with an output power of 80 watts. A delta antenna with a 40-meter base and a 15-meter apex was used at each station with the plane of the antenna in an east-west direction. The two transmitter sites operated with transmitting frequencies separated by 20 Hz so that both frequencies would simultaneously pass through the receiver IF-filters.

Each of the receiver sites had Racal 6790gm receivers. The receivers were set in cw mode with a selectivity of less than 400 Hz. The receivers were tuned 10 Hz below the lowest transmitter frequency with a -30 Hz BFO frequency that produced an output of +40 and +60 Hz for the two received frequencies. The receiver outputs were recorded on one channel of four track analog tape recorders. A 60 Hz time code was recorded on another track of the recorders so that a time reference was available for analysis.

Table 2
Reflection Point Parameters

Link	Radial Distance	Compass* Direction	$\vec{k} \cdot \vec{B}$
Mountainair to Stallion Range	65 km	-1°	-.58
Mountainair to Monte Vista	268 km	$+5^{\circ}$	.30
Los Alamos to Stallion Range	146 km	$-30'$	-.13
Los Alamos to Monte Vista	340 km	$+4^{\circ}$	.40
Taos to Stallion Range	169 km	$+10^{\circ}$	.14
Taos to Monte Vista	375 km	$+8^{\circ}15'$	.48
Pagosa Springs to Stallion Range	191 km	$-8^{\circ}15'$	
Pagosa Springs to Monte Vista	418 km	-2°	

*Direction from ground zero

Magnetic Inclination 61°
Magnetic Declination $+31^{\circ}$

SECTION 3

DATA ANALYSIS

3-1 VERTICAL INCIDENCE PHASE SOUNDING

Ionospheric changes due to either density changes or bulk motion will result in the phase of the reflected signal changing relative to the phase of the input waveform of the transmitter. On an oscilloscope trace of the return pulse, relative phase changes appear as a waveform moving across the pulse envelope. Figure 2 shows the position of the peaks of the wave forms in the pulse envelope as time progresses. The ocilloscope trace is along the ordinate and the abcissa corresponds to different traces, or equivalently the passage of time. A locus of points with zero slope corresponds to a constant phase path whereas a nonzero slope indicates an ongoing phase path change. In fact the slope is proportional to the doppler impressed on the transmitted signal, i.e.,

$$f(\text{doppler}) = k\tan^{-1}(\theta) \ .$$

Theta is the angle of the particular trace with respect to the horizontal. The scale factor k depends on the ratio of sweep time of the oscilloscope trace to the speed of the film moving across the scope face. For our system the value of k was 0.79.

Figures 3,4 and 5 show the doppler obtained for the three operating frequencies. These were arrived at by measuring the slope of the phase traces with respect to time. Since the slope was measured from the hard copy and the traces are not smooth curves, an uncertainty of approximately two degrees is introduced. This becomes a 15% uncertainty for the largest doppler values. Because of the ionospheric profile on shot day and the selected operating frequencies, the Ordinary (O) and Extraordinary (X) modes of propagation were not resolved in the return echoes. However, because the O and X mode reflections occur at differing ionospheric heights, the onset of an upward propagating disturbance affects the X-mode return before the O-mode. This feature allows us to visually separate the two modes on the data traces. The doppler plots in figures 3 to 5 are for O-mode returns.

3-2 BISTATIC SYSTEM.

The doppler shift of the received signal from a particular transmitter is a measure of the ionospheric motion at the reflection point. We have taken two different approaches to deriving the doppler shift from the recorded data. Both have some drawbacks. The most direct measurement of the doppler is to play the analog data from the recorder through a hardwire spectrum analyzer and produce plots of power spectra versus time on a film, using gray scales to represent the magnitude of power. This method allows us to look at side bands of the main carrier which may contain information on ionospheric motions via propagation paths that contain little power. However this method does not have adequate frequency resolution to identify small disturbances.

Digitization of the analog data and processing by a computer provides the most complete and flexible data analysis. We employ a complex demodulation procedure to separate the composite signal from the two transmitters into two components. The average phase of each of these signals is then computed and displayed (reference 2). More sophisticated frequency analysis is possible for obtaining information on the sidebands present in the signal.

SECTION 4

RESULTS

4-1 VERTICAL SOUNDER.

The arrival of the shock wave from the explosion is clearly visible on all three frequencies (see figures 2-4). The passage of the shock wave gives rise first to a positive doppler followed by a negative doppler and then another positive doppler. This shape is caused by the shock wave initially producing a lowering of the ionospheric reflection level by compression, then a raising of the reflection level as a result of the passage of the rarefaction behind the shock front, and finally a return to the steady state reflection height (reference 3).

Because the propagation of an acoustic pulse in the ionosphere is nonlinear, a shock wave is formed that is shaped much like an "n". As a result, detailed structure in the original acoustic signal is lost and the only causal nexus between the original pulse and the final shape appears to be provided by the energy density and the spatial extent. The quantities that are therefore of interest are the arrival time of the shock front, the magnitude of the disturbance and the duration. Figures 2, 3 and 4 show a comparison between theory and experiment (reference 4). The lack of correspondence between the predicted and measured arrival times may be accounted for by the lack of detailed information on the sound speed versus height. Additionally the shock front velocity is not incorporated in the calculation and may lead to an underestimation of the propagation velocity. The difference between theory and experiment for the maximum doppler shifts and the pulse durations cannot be accounted for by uncertainties in the data or yield of the explosion. Again sound speed uncertainties may account for the underestimation of the period while the lack of incorporation of dissipative mechanisms in the computer model may explain the overestimation of the doppler shifts.

4-2 BISTATIC SYSTEM.

The magnitudes of the observed doppler shifts range from 0.1 Hz to approximately 3 Hz. The magnitude of the noise is less than 0.05 Hz, but multipath fading obscured signals of less than 0.1 Hz. The disturbance can be seen on several of the doppler plots as a positive, then negatively going frequency shift of about one minute in duration. This corresponds to the prompt acoustic pulse propagating through the ionospheric reflection region. The arrival time of the acoustic pulse can be inferred from the ray trace calculation shown in figure 5. There is some discrepancy of the predicted arrival time versus the observed times, possibly due to uncertainties in the atmospheric parameters used and the presence of ionospheric winds. A response of the ionosphere to the acoustic pulse is seen as far away as the Taos to Monte Vista reflection point. It can be inferred from the acoustic ray trace plot that a weak disturbance should be detected at the altitude and distance of this reflection point.

By far the most dramatic signal was seen for the Stallion Range to Mountainaire link with a reflection point 65 km from ground zero. Figure 6 shows the doppler plot obtained direcly by the spectral analysis of the analog signal. Note that there are two distinct components to the signal, one an X-mode and the other an O-mode reflection. Because the X-mode ray path reflects nearly the source, the response is seen first on the X-mode component followed by the more distant O-mode reflection.

Because of the weak signals on the other bistatic links, we applied digital signal processing techniques. Figures 7 through 12 are plots of the observed doppler shifts calculated from the data obtained at the Mountainair, Los Alamos and Taos receivers. Data from the Pagosa Springs station has not yet been processed because of the poor quality of the recording.

The large doppler fluctuation that is seen on the Mountainair plot appears to be too early for the propagating acoustic disturbance to reach the nominal reflection point. This signal is probably due to a large portion of the link power coming from an off path reflection closer to ground zero. Such a path may be a double hop or a single hop from a tilted ionosphere. There are indications that this same phenomena occurs on the other links if one looks at the frequency sidebands of the carrier. One interesting feature is the lack of a response on the Taos to Stallion Range link, and a lack of a response at the proper time for the Mountainair to Monte Vista links, even though the reflection points are closer to the acoustic source than the Taos to Monte Vista point where a response was seen. It may be that the coupling between the neutral pulse and the electrons is very weak for these links because the orientation of the acoustic propagation vector with respect to the ambient magnetic field at the rf reflection region is not favorable. The values of these coupling strengths, assuming no ionospheric winds, are listed in Table 1. Ionospheric winds could have a marked effect on these values by changing the direction of the propagation vector. The data from a SRII experiment indicate that there were winds from the west (reference 5).

The Los Alamos to Monte Vista link has a response that consists of the expected acoustic disturbance and a precursor that arrives about two minutes earlier. The origin of this precursor is not understood and is not likely a multi-hop path, because the phase of the disturbance is opposite to the expected phase. Another phenomenon that is seen in figures 11 and 12 is the significant reduction of multipath interference fading for a period of several minutes around the arrival time of the acoustic pulse. This apparently occurs because of the interruption of the sencondary ray-paths. The reason for the presistent interruption is under study.

SECTION 5

SUMMARY

The observation of the acoustic pulse passing through the ionosphere from the MILL RACE experiment is consistent with the predictions of our acoustic and radio propagation codes. The exact form of the disturbance near the explosion is also very close to the predicted shape. There still is uncertainty concerning many of the details of the observations at the remote sites. These observations require further study.

ACKNOWLEDGMENTS

This research was performed under the auspices of the US Department of Energy, International Security Affairs research and development program. Field support at White Sands Missle Range was provided by the Field Command of the Defense Nuclear Agency.

REFERENCES

1. Bernhardt, Paul, A Study of Coupling Between the Neutral Air Motion and the Ionosphere, LAMS report to be published, Los Alamos National Laboratory.

2. Fitzgerald, T. J., Numerical Techniques for CW RF Doppler Analysis. S(cience) E(ngineering) A(ssociates) report, to be published. SEA Albuquerque, NM.

3. Hall, C. J., Nuclear Weapon Detection by Radio Techniques, SSDS1/70, AWRE.

4. Warshaw, Stephen I., On a Finite Amplitude Extension of Geometric Acoustics in a Moving Inhomogeneous Atmosphere, UCRL 53055, Lawrence Livermore National Laboratory.

5. Chaing, Norman, Private Communication, SRI Menlo Park, CA.

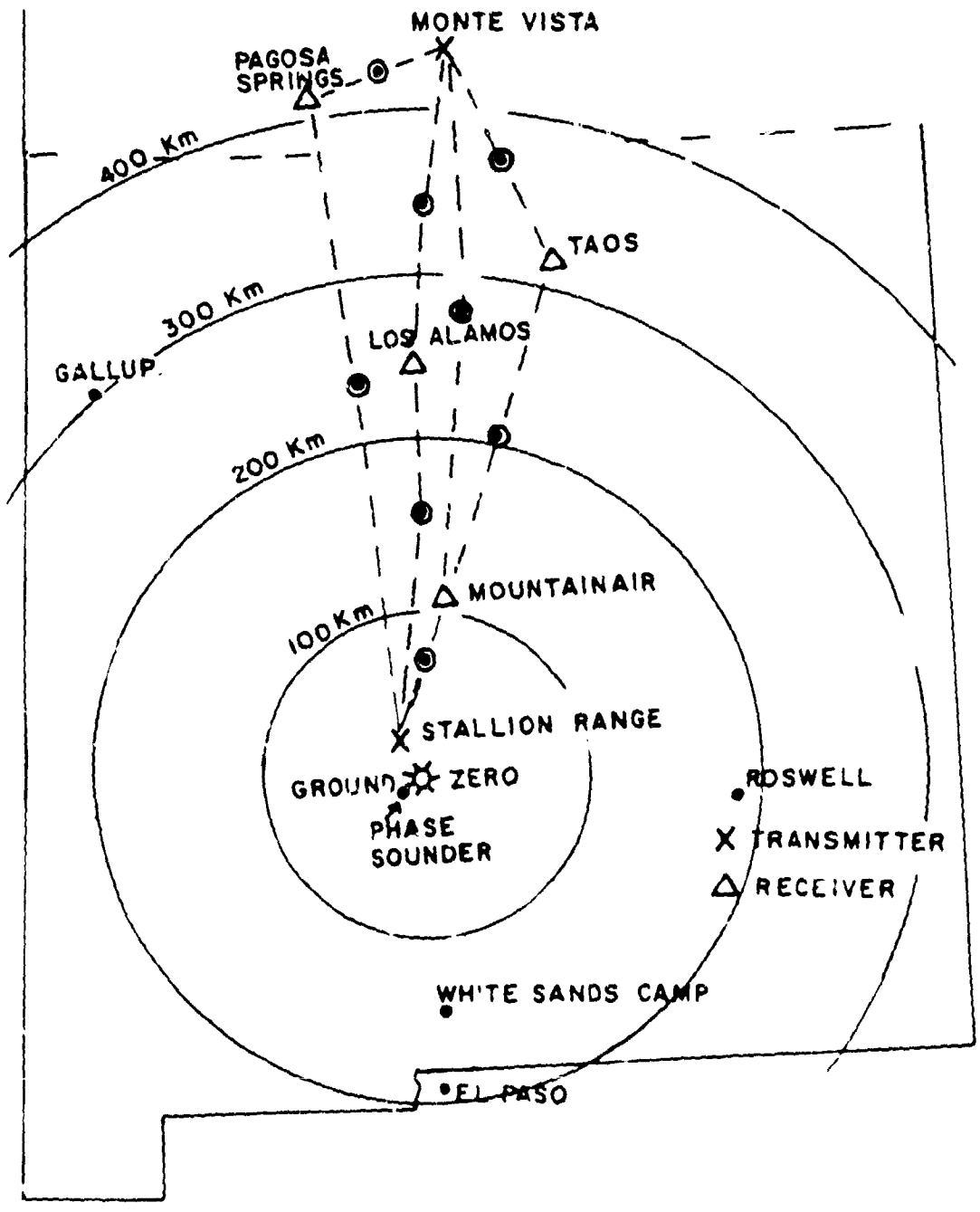

FIGURE 1. Locations of sounding instruments for MILL RACE experiment. "x"s are the transmitter sites, triangles are the receiver sites and the "bulls eyes" are the ionospheric reflection points.

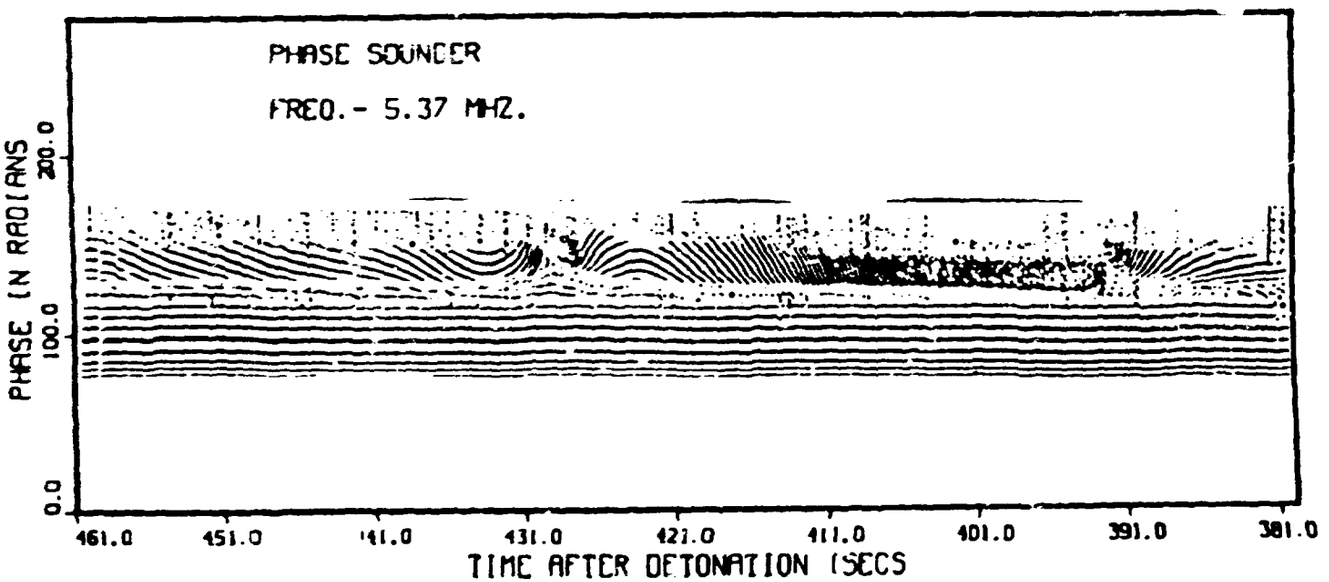

FIGURE 2. Typical range-time-intensity plot produced by the vertical incidence sounder.

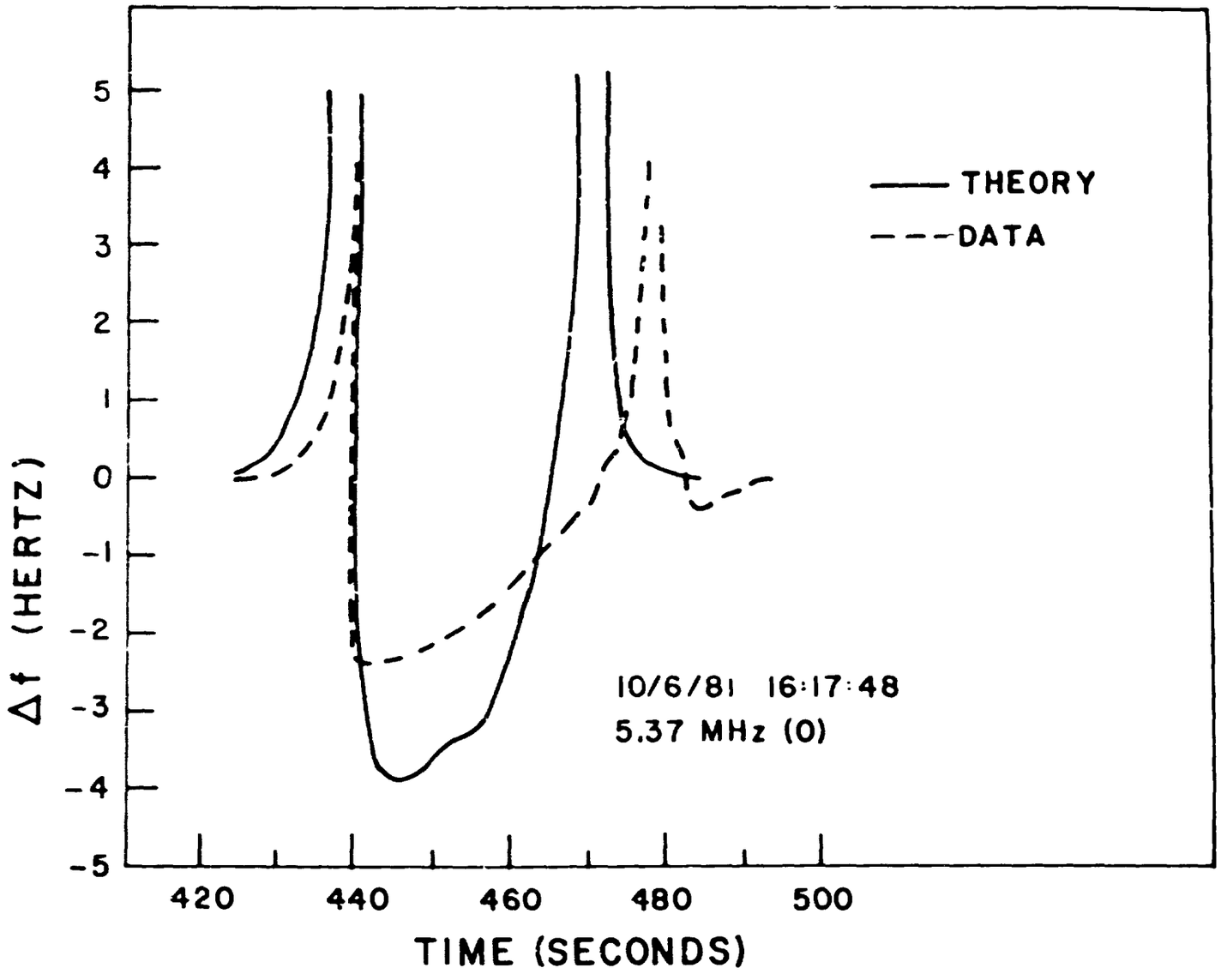

FIGURE 3. Observed doppler shift at 5.37 Mhz recorded by the phase sounder near ground zero.

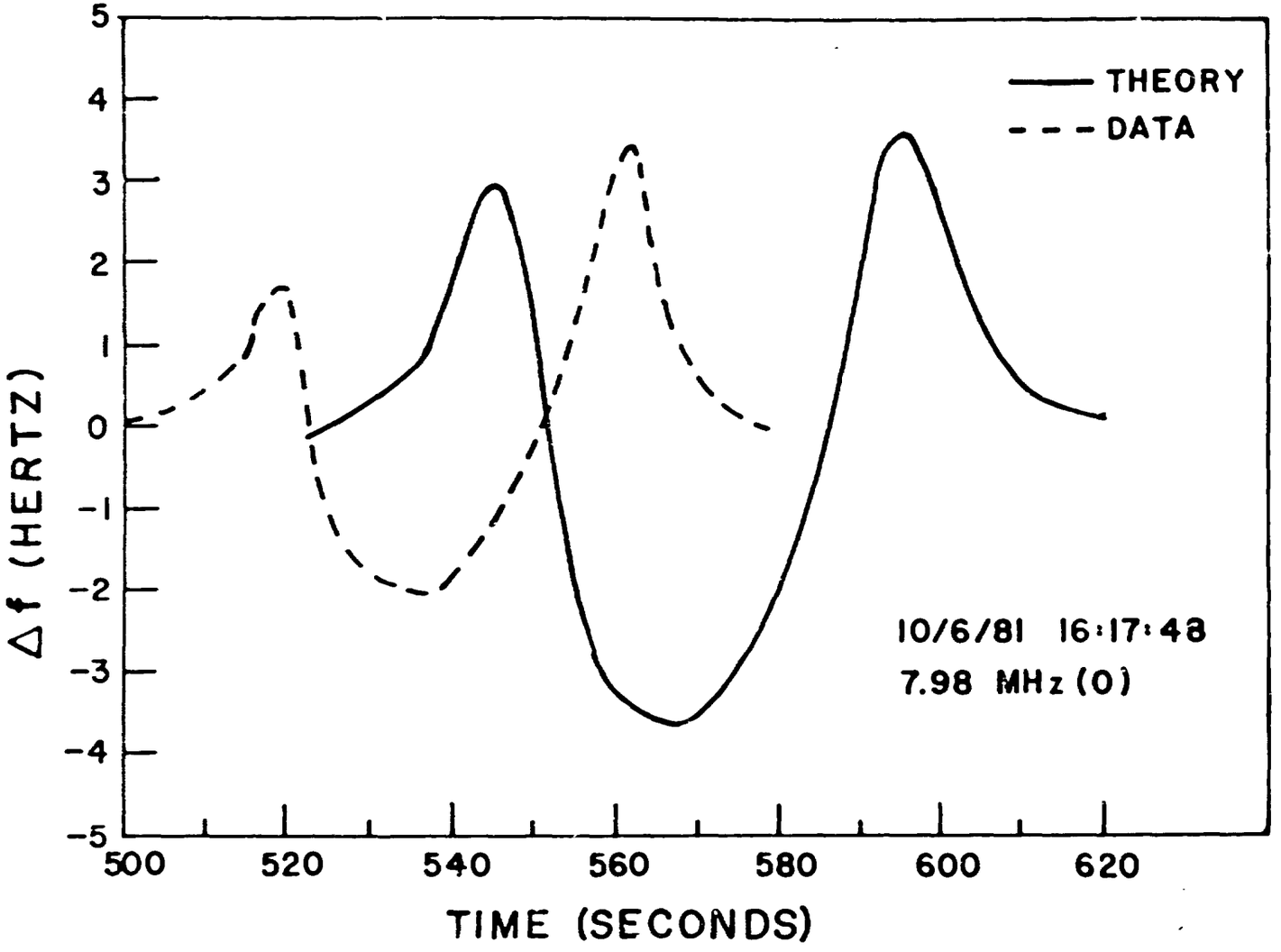

FIGURE 4. Observed doppler shift at 7.98 Mhz recorded by the phase scunder near ground zero.

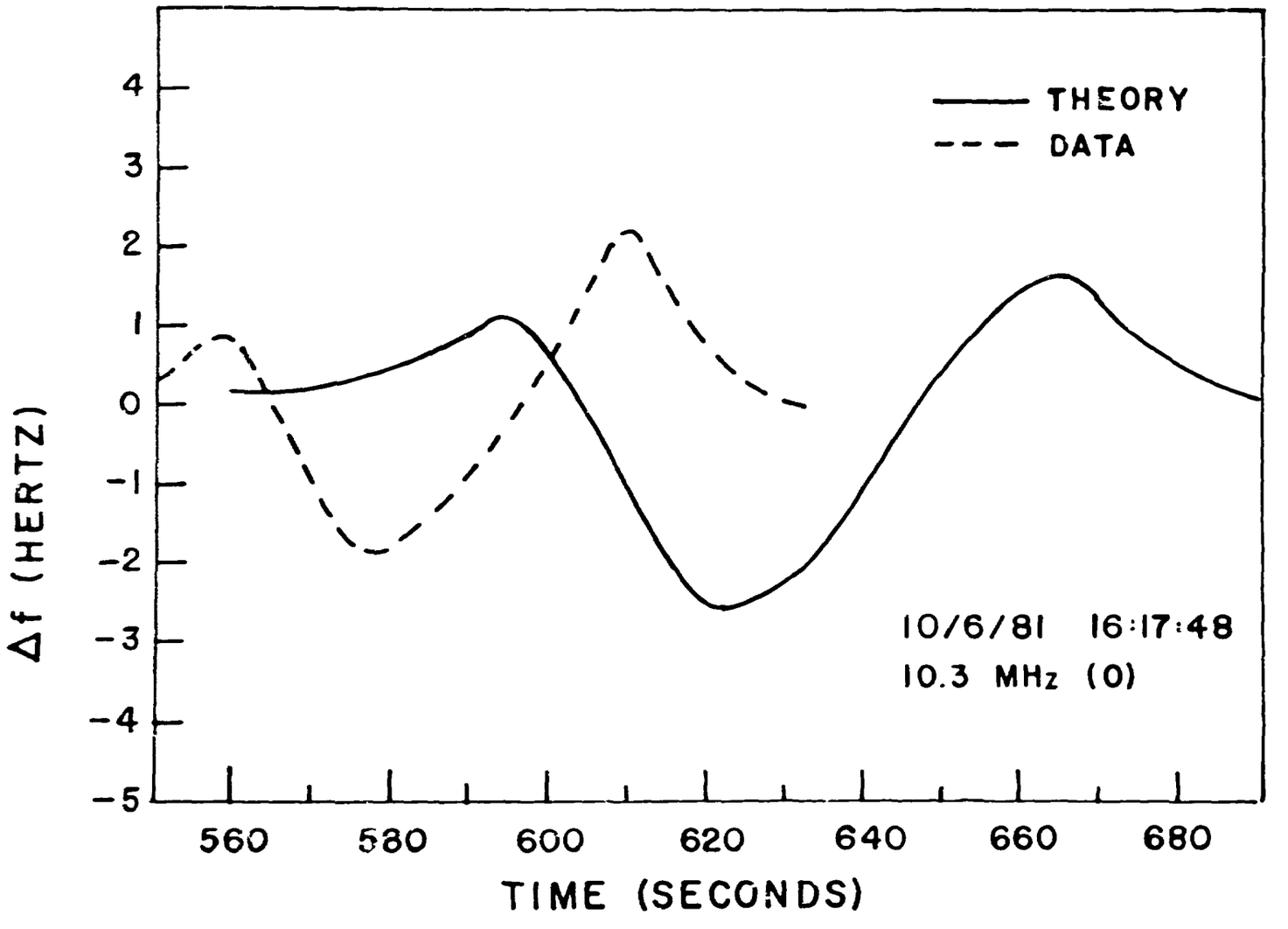

FIGURE 5. Observed doppler shift at 10.3 Mhz recorded by the phase sounder near ground zero.

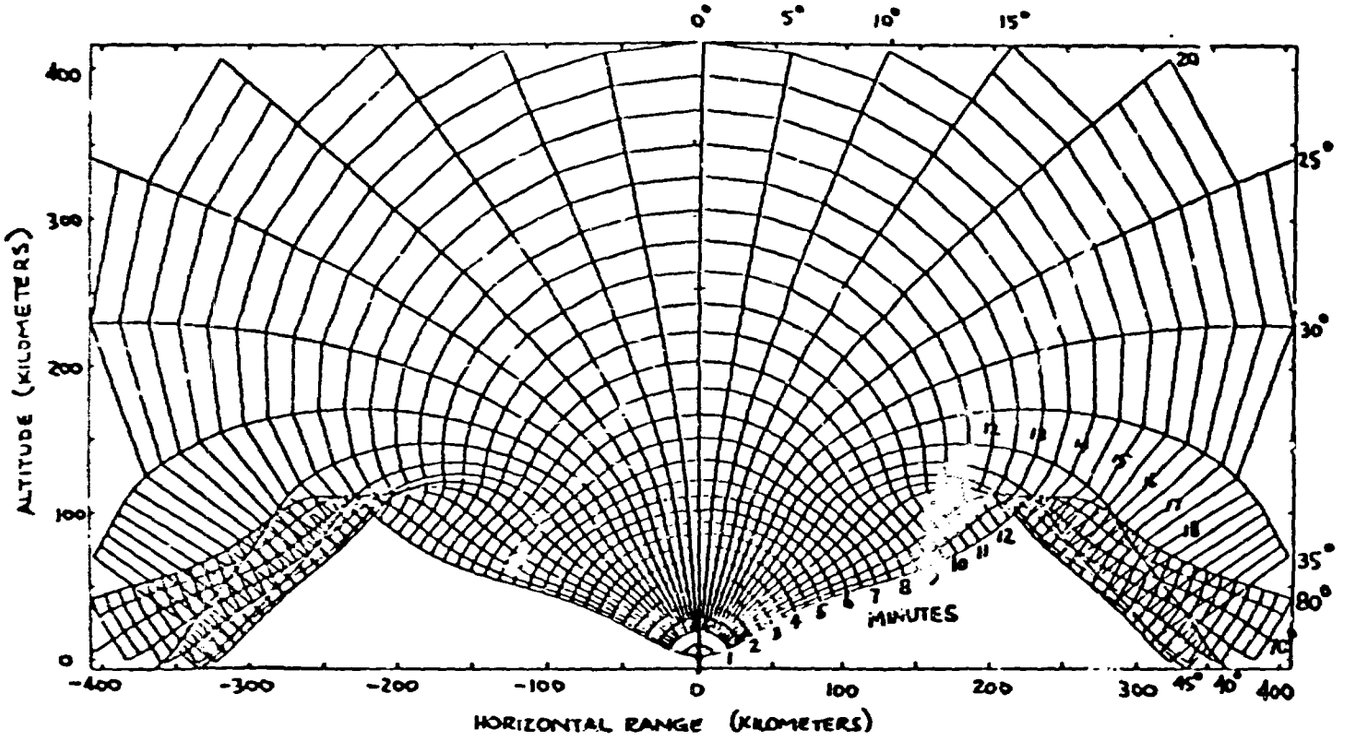

FIGURE 6. LLNL-calculated acoustic ray paths and wavefront surfaces for surface H.E. blast (linear theory, point explosion).

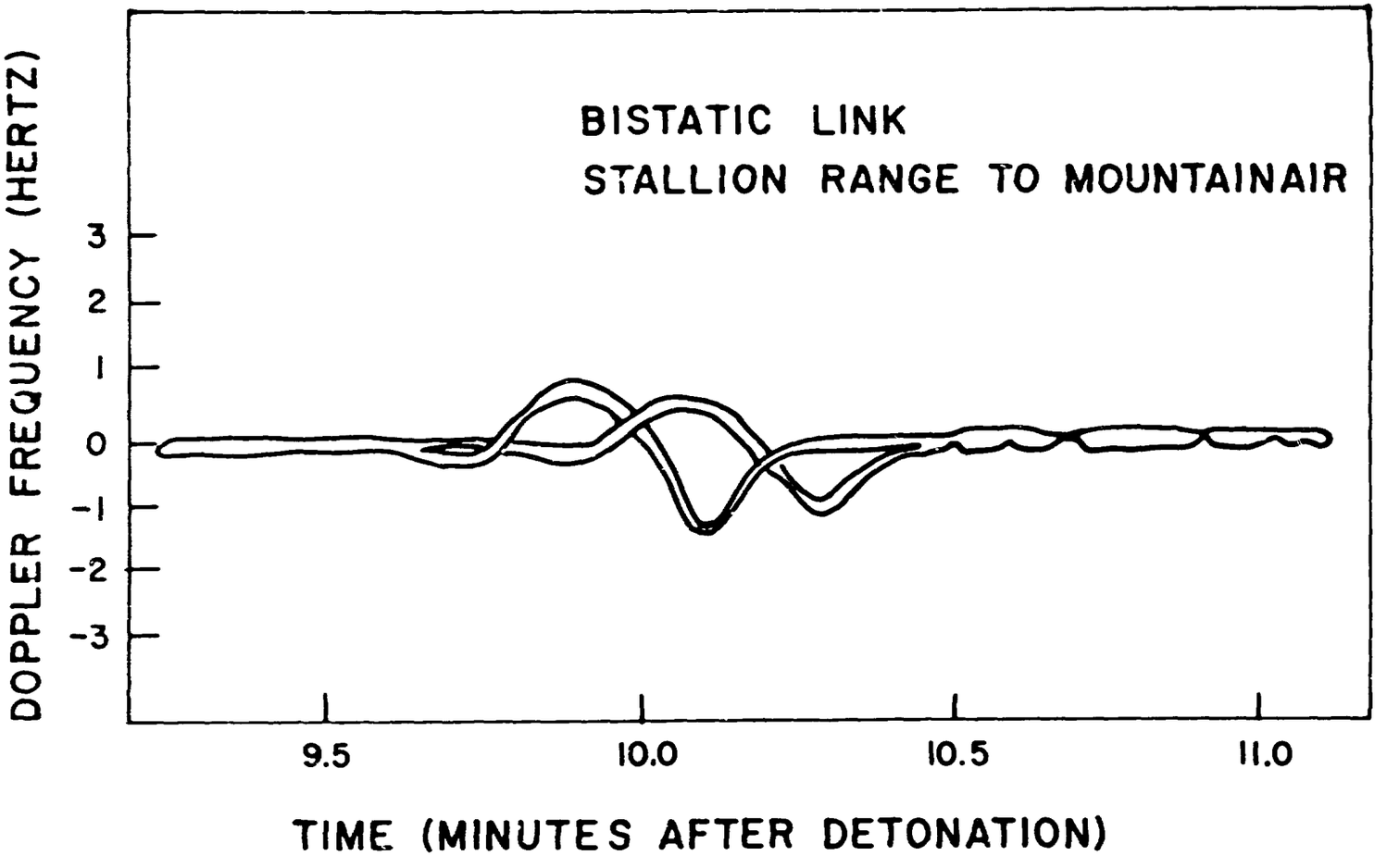

FIGURE 7. Doppler plot from spectrum analyzer for the Stallion Range to Mountainair link.

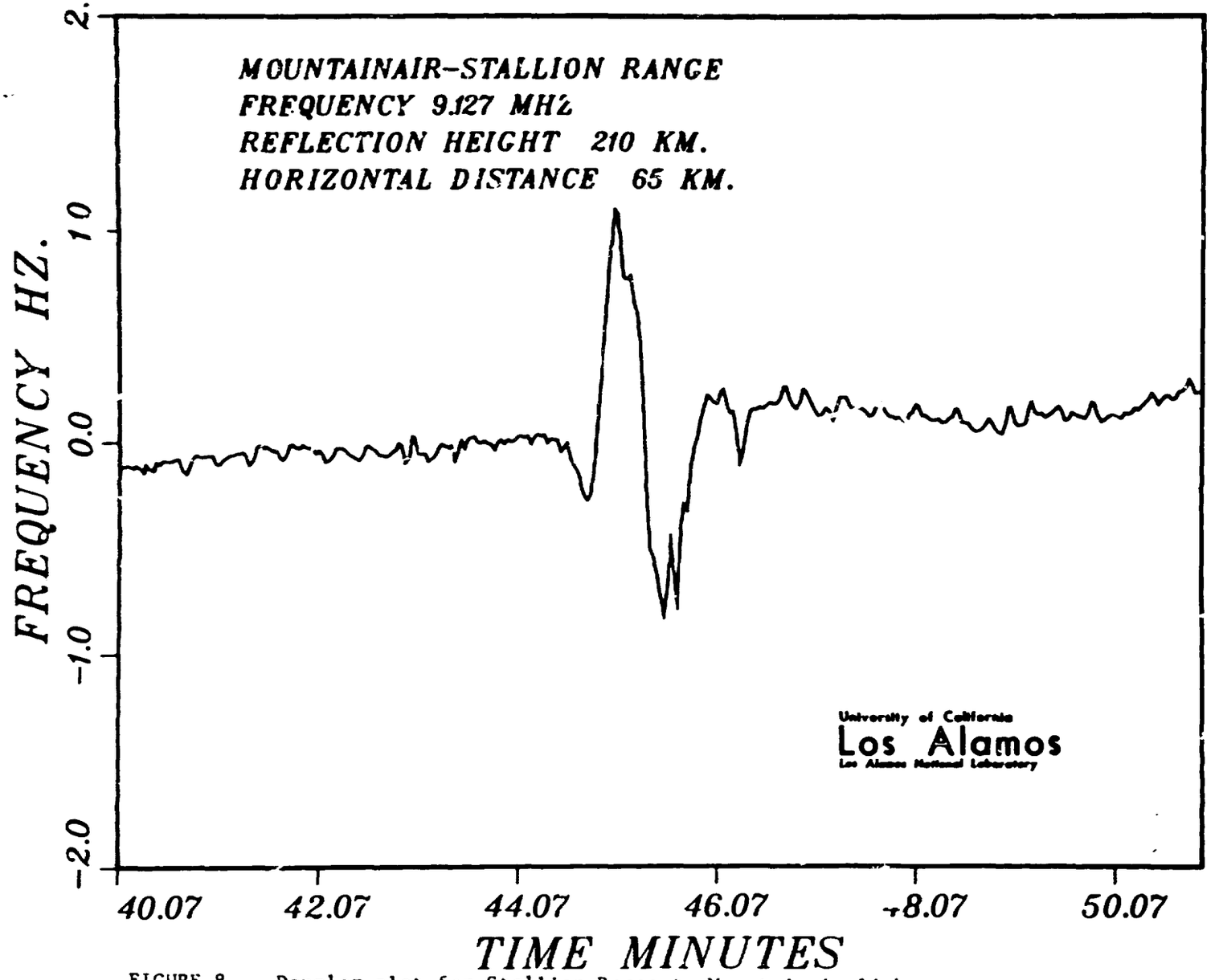

FIGURE 8. Doppler plot for Stallion Range to Mountainair link produced by digital analysis.

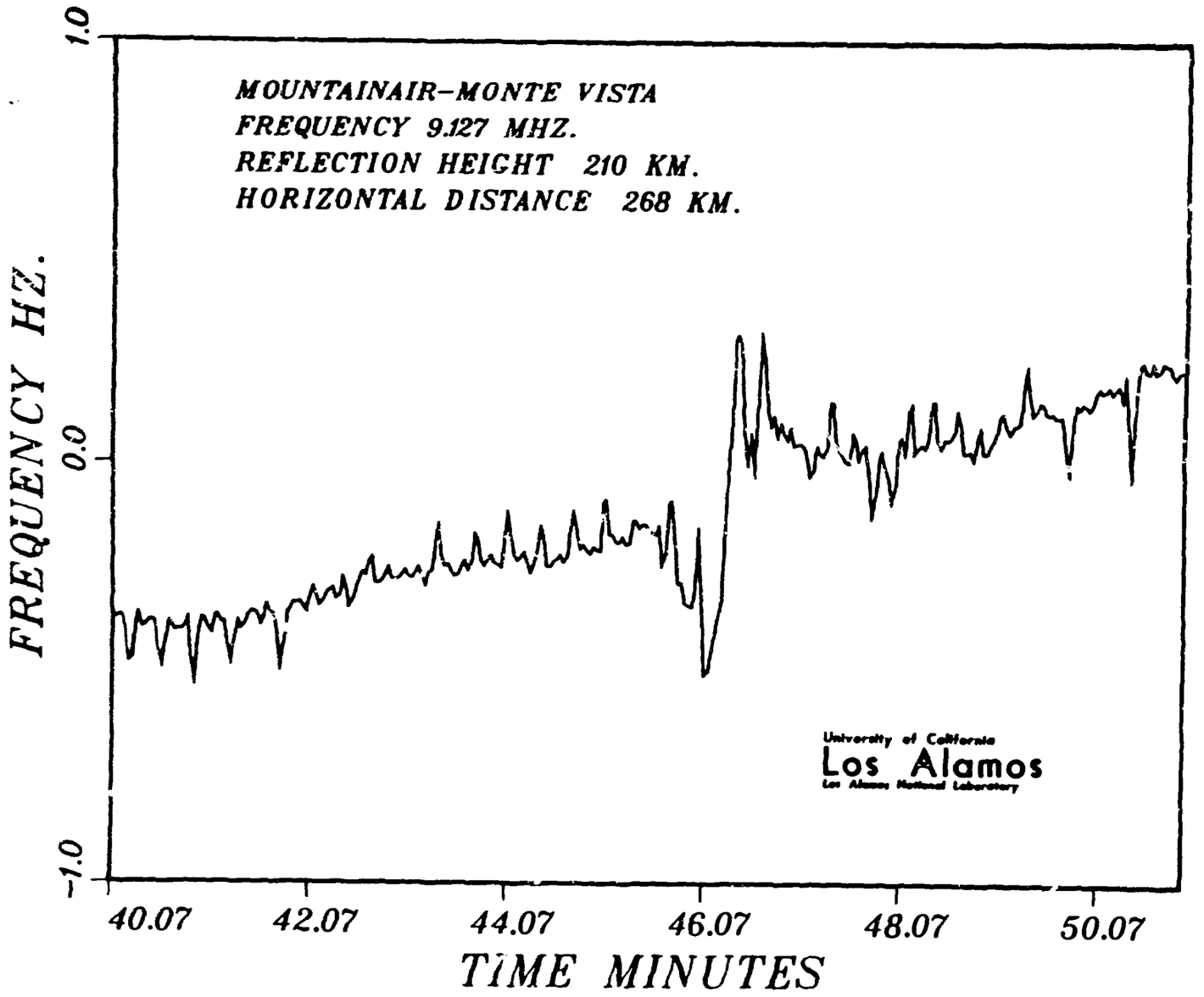

FIGURE 9. Doppler plot for Monte Vista to Mountainair link.

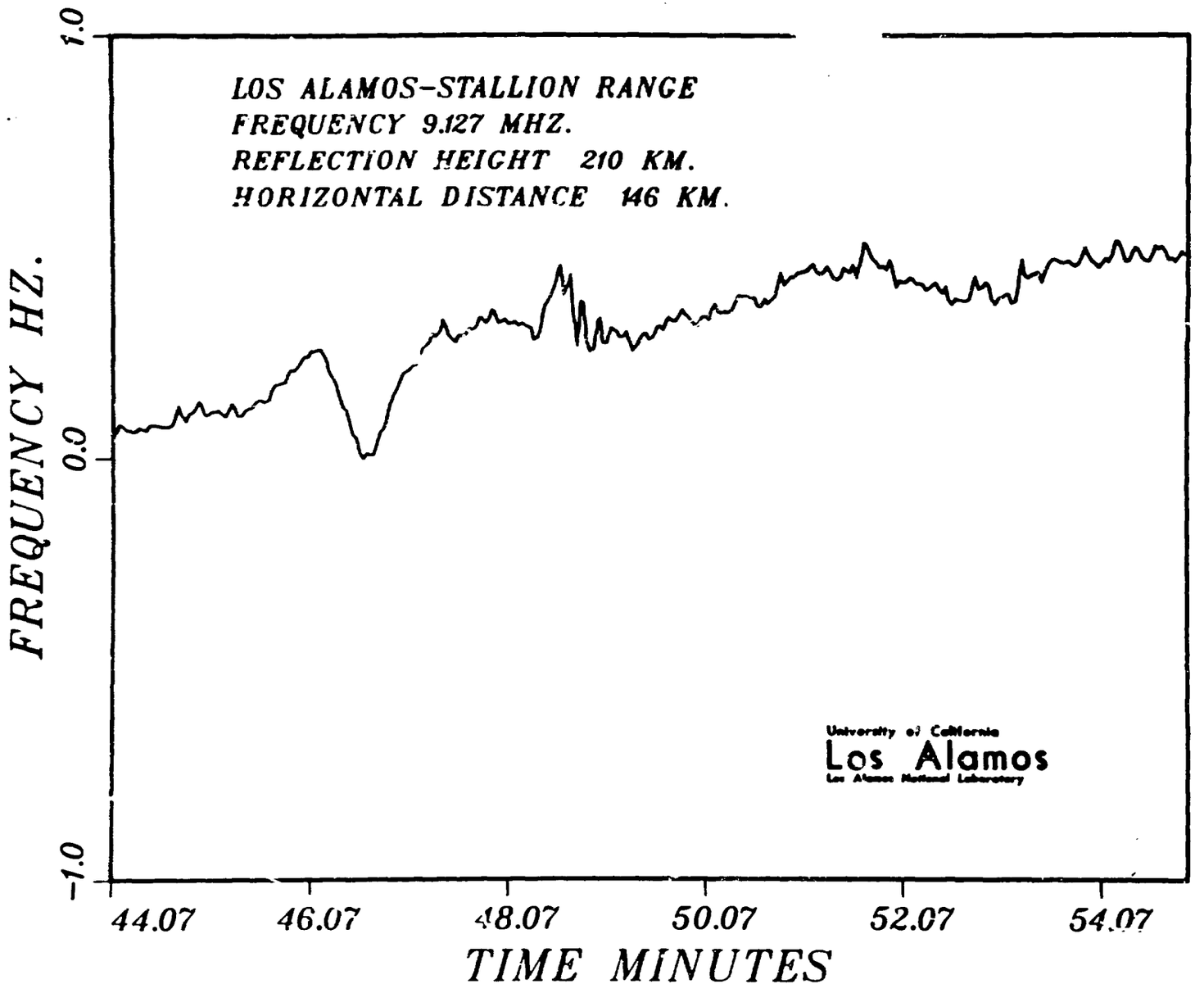

FIGURE 10. Doppler plot for Stallion Range to Los Alamos link.

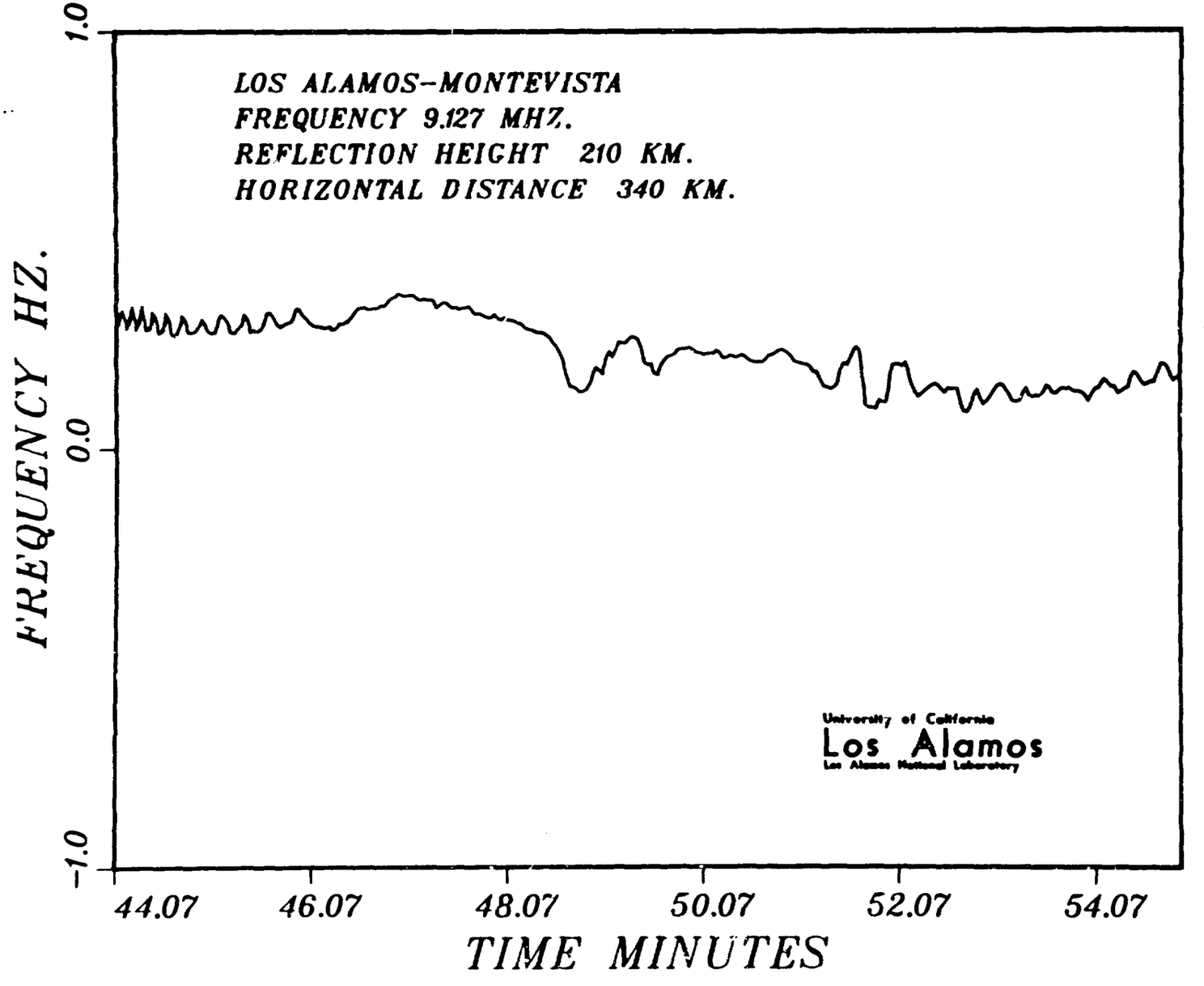

FIGURE 11. Doppler plot for Monte Vista to Los Alamos link.

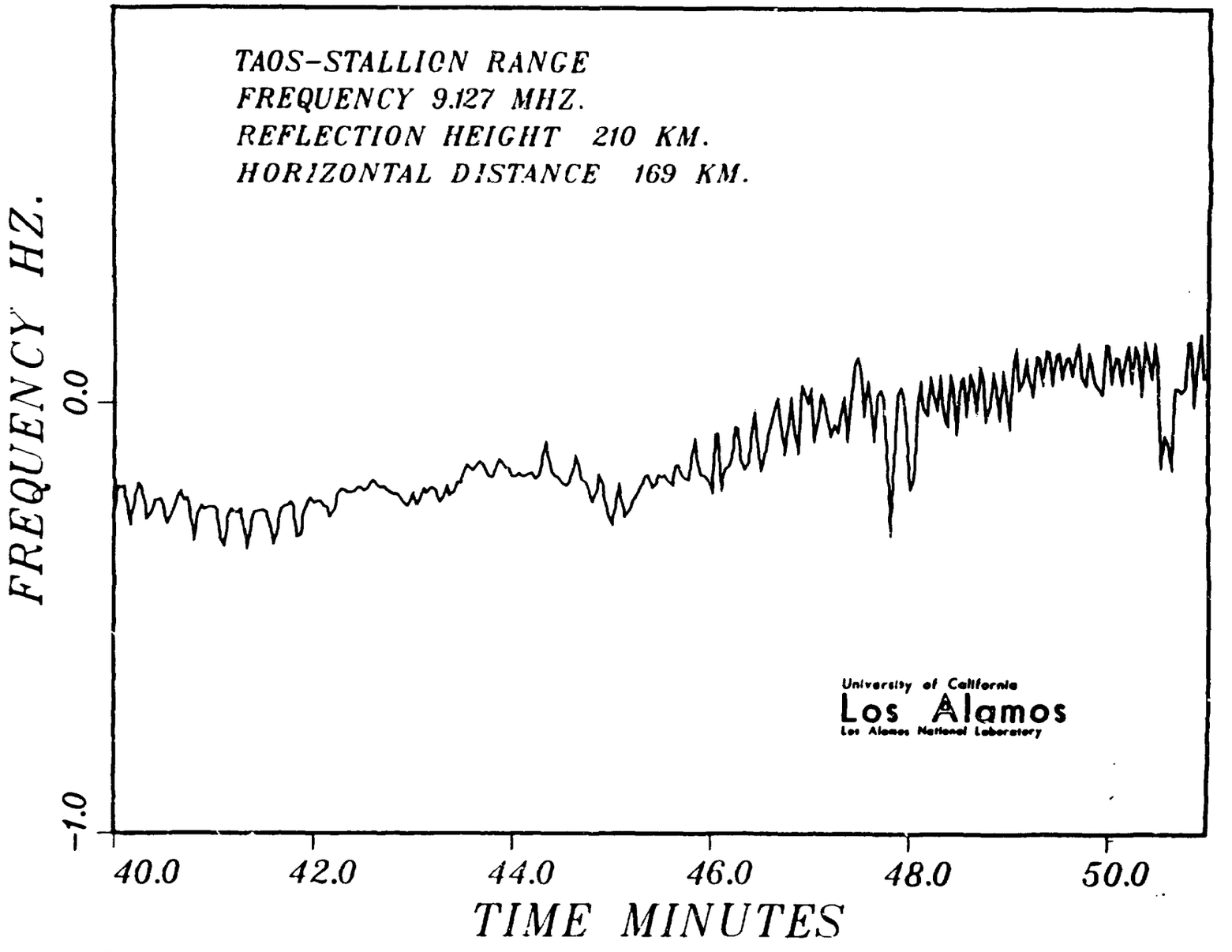

FIGURE 12. Doppler plot for Stallion Range to Taos link.

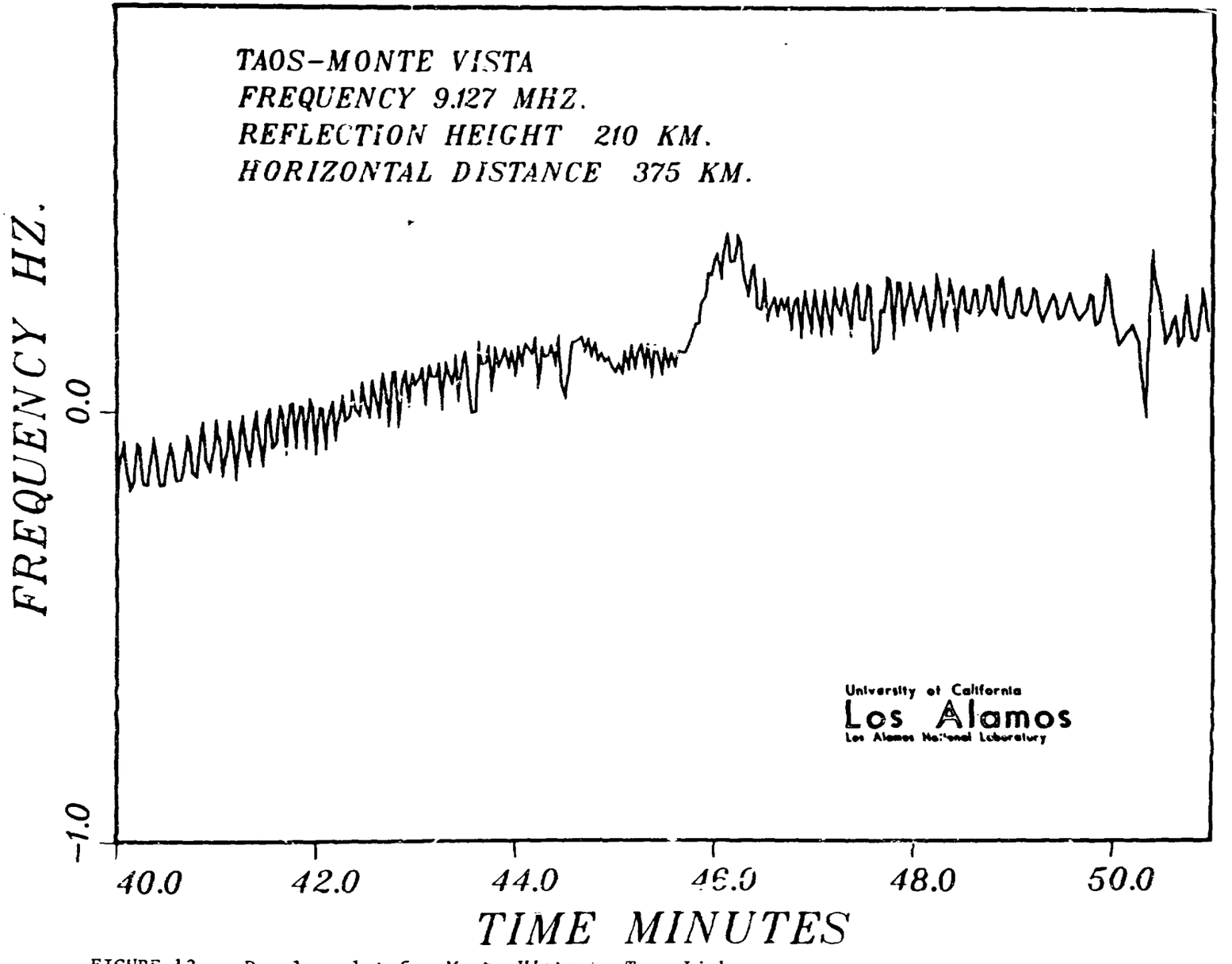

FIGURE 13. Doppler plot for Monte Vista to Taos Link.